

Promotion of Tubulin Assembly by Aluminum Ion in Vitro

TIMOTHY L. MACDONALD, W. GRIFFITH HUMPHREYS,
R. BRUCE MARTIN

It has been proposed that aluminum ion is a contributing factor in a variety of neurological diseases. In many of these diseases, aberrations in the cytoskeleton have been noted. The effects of aluminum ion on the *in vitro* assembly of tubulin into microtubules has been examined by determining the association constants for the metal ion–guanosine triphosphate–tubulin ternary complex required for polymerization. The association constant for aluminum ion was approximately 10^7 times that of magnesium ion, the physiological mediator of microtubule assembly. In addition, aluminum ion at 4.0×10^{-10} mole per liter competed effectively with magnesium ion for support of tubulin polymerization when magnesium ion falls below 1.0 millimole per liter. The microtubules produced by aluminum ion were indistinguishable from those produced by magnesium ion when viewed by electron microscopy, and they showed identical critical tubulin concentrations for assembly and sensitivities to cold-induced depolymerization. However, the rate of guanosine triphosphate hydrolysis and the sensitivity to calcium ion–induced depolymerization, critical regulatory processes of microtubules *in vivo*, were markedly lower for aluminum ion microtubules than for magnesium ion microtubules.

ALUMINUM ION (Al^{3+}) HAS BEEN proposed as a factor contributing to a variety of neurological and skeletal disorders, including an encephalopathy and a type of osteomalacia observed in patients with chronic renal failure on long-term hemodialysis (1). The high prevalence of amyotrophic lateral sclerosis and a form of Parkinsonian dementia in areas where the soil has a high Al^{3+} content, with simultaneous low magnesium (Mg^{2+}) and calcium ion (Ca^{2+}) contents, has implicated this metal ion imbalance and specifically Al^{3+} as a neurotoxic agent (2). High Al^{3+} concentrations occur in the nuclear region of neurofibrillary tangle-bearing neurons of the hippocampus in brain tissue from patients with Alzheimer's disease, but it is not known whether Al^{3+} is etiologically related to the disease or has an affinity for these abnormal neural regions (3).

Aluminum ion is released from mineral stores by acid rain (4). Because of the enhanced exposure to Al^{3+} and its potential for human toxicity, we have been examining the effects of Al^{3+} on biological systems *in vitro*. We have developed a kinetic method to determine the association constant of the metal ion–guanosine triphosphate–tubulin ternary complex required for microtubule

assembly and have found that Al^{3+} is a potent initiator of tubulin polymerization, having an association constant approximately 10^7 times that of Mg^{2+} , the physiological mediator of microtubule assembly. In addition, the rate of guanosine triphosphate hydrolysis and the sensitivity to calcium ion–induced depolymerization, critical regulatory processes of microtubules *in vivo*, were markedly lower for Al^{3+} microtubules than for Mg^{2+} microtubules.

Aluminum ion, when injected into the brains of experimental animals, causes the formation of cytoskeletal lesions composed primarily of intermediate filaments, known as neurofibrillary tangles (5). Neurofibrillary tangles can be induced by a variety of neurotoxic agents, which are thought to

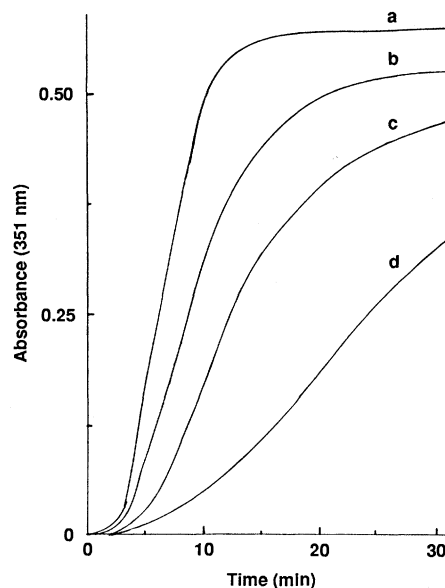


Fig. 1. Microtubule assembly initiated by Al^{3+} monitored by measuring turbidity at A_{351} . The assembly conditions were MAP-free tubulin ($20 \mu M$), GTP ($1.0 mM$), DMSO (8% by volume), and various Al^{3+} concentrations calculated by Eq. 2. Curve a, $[Al^{3+}] = 1.3 \times 10^{-11} M$; curve b, $[Al^{3+}] = 1.5 \times 10^{-12} M$; curve c, $[Al^{3+}] = 7.0 \times 10^{-13} M$; curve d, $[Al^{3+}] = 2.7 \times 10^{-13} M$. These results are from a single isolation of tubulin, which provides high reproducibility ($\pm 3\%$).

operate by disrupting the cytoskeleton at several loci. One target site for these agents is the microtubular system. The assembly of tubulin, the principal subunit of microtubules, requires Mg^{2+} , which is thought to bind at receptor sites for guanosine triphosphate (GTP) and guanosine diphosphate (GDP), and is inhibited by Ca^{2+} , which is believed to associate at a distinct binding site (6). Thus, tubulin represents a potential site through which the aberrant physiological processes induced by Al^{3+} could be mediated.

Tubulin, free of microtubule-associated proteins (MAPs), was prepared from bovine brain by three cycles of assembly and disassembly and stored in aliquots in liquid nitrogen (7). Before being used, the frozen protein was rapidly thawed, centrifuged at $5000g$ for 10 minutes to remove small amounts of denatured protein, and then chromatographed on a Sephadex G-50 (fine) column equilibrated with $0.1M$ 1,4-piperazine diethanesulfonic acid (Pipes) buffer (pH 6.9). Protein concentrations were determined by the method of Bradford and calibrated with tubulin as a standard (8). Tubulin, in the metal- and GTP-free buffer, degenerated rapidly by first-order kinetics ($k = 3.4 \times 10^{-3} \text{ min}^{-1}$); thus, all experiments had to be conducted within 2.5 hours after the protein was initially thawed. Each experiment was corrected for protein denaturation through the use of standard polymerization assays conducted before and after each set of experiments. Tubulin assembly was initiated by the addition, at $4^\circ C$, of a solution of tubulin (sufficient to produce a final concentration of $20 \mu M$ tubulin) to a solution prepared by the sequential addition of the appropriate metal ion concentration, GTP (to a final concentration of $1.0 mM$), and Pipes (to a final concentration of $100 mM$), and dimethylsulfoxide (DMSO) (to a final volume of 8.0%) (9). The solution was placed in a microcuvette equilibrated at $37^\circ C$, and the course of tubulin polymerization was monitored in the elongation phase by measuring the increase in light absorption at 351 nm (10) with a spectrophotometer (Varian DMS 90 UV-Vis) (Fig. 1). The microtubules produced by Al^{3+} and Mg^{2+} initiation were identical when examined by electron microscopy (Fig. 2). In addition, the critical concentrations of Al^{3+} and Mg^{2+} required to initiate polymerization were identical (Fig. 3), and the sensitivities of microtubules induced by the two ions to cold-induced depolymerization were indistinguishable.

The rate of microtubule formation was

Department of Chemistry, University of Virginia, Charlottesville, VA 22901.

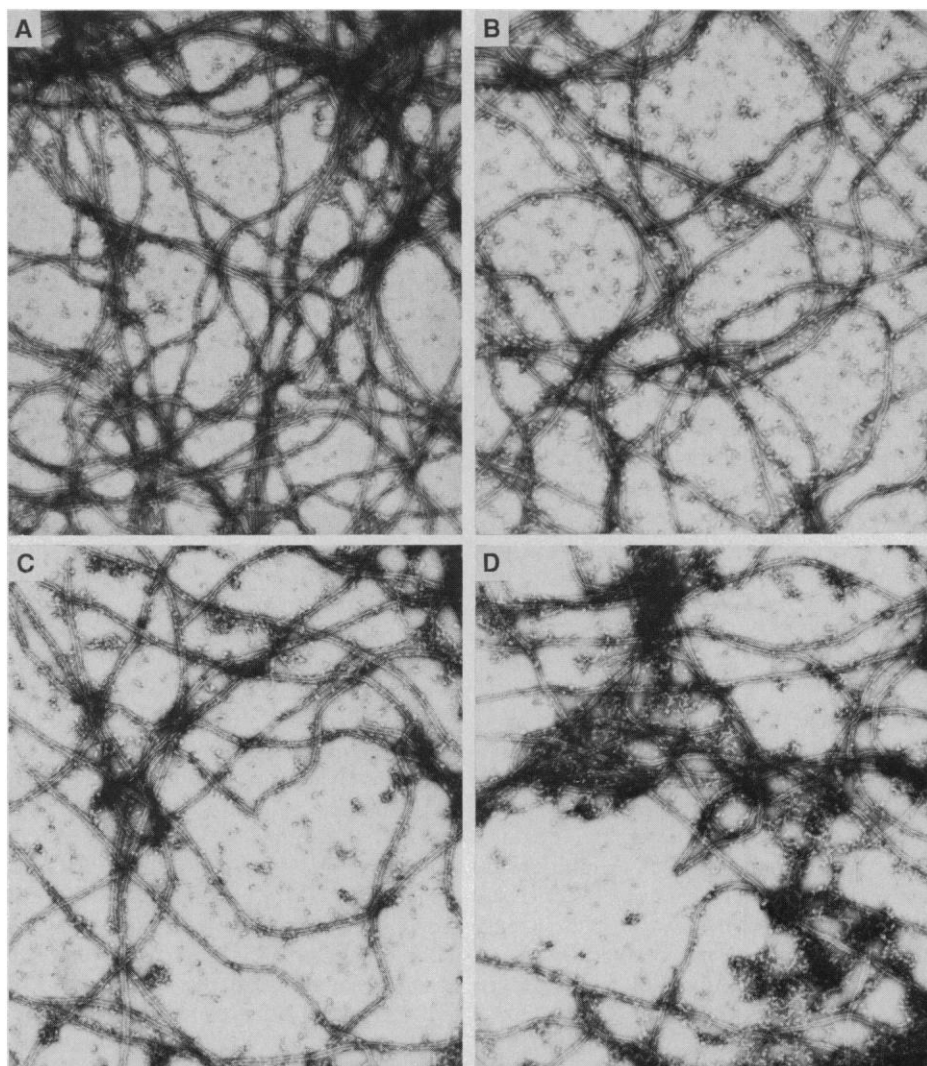


Fig. 2. Transmission electron micrographs (Hitachi HU-11) of microtubules initiated by either Al^{3+} or Mg^{2+} ($\times 16,000$). The polymerized samples were fixed with glutaraldehyde (1%), placed on carbon-coated grids, then negatively stained with uranyl acetate (1%). All samples contained GTP (1.0 mM), Pipes (100 mM), and the following: (A) MAP-free tubulin (2.0 mg/ml, 20 μM), DMSO (8% by volume), NTA (2.0 mM), and $\text{AlCl}_3 \cdot (\text{H}_2\text{O})_6$ (1.0 mM) = $[\text{Al}^{3+}]$ of $4.0 \times 10^{-11}\text{M}$; (B) MAP-free tubulin (2.0 mg/ml, 20 μM), DMSO (8% by volume), MgSO_4 (1.0 mM); (C) MAP-containing tubulin (2.0 mg/ml), NTA (2.0 mM), and $\text{AlCl}_3 \cdot (\text{H}_2\text{O})_6$ (1.0 mM) = $[\text{Al}^{3+}]$ of $4.0 \times 10^{-11}\text{M}$; (D) MAP-containing tubulin (2.0 mg/ml) and MgSO_4 (1.0 mM).

related to the association constant of the metal ion with the GTP-tubulin complex. Since we verified by electron microscopy the absence of other large structures that scatter light (Fig. 2), metal ion-dependent formation of microtubules could be monitored by the apparent absorption at 351 nm. Such absorption represents the turbidity, which for thin, rigid microtubule rods longer than the wavelength of light monitors the weight fraction of protein units appearing as polymer (11). For the usual elongation kinetics (12), the turbidity becomes proportional to $1 - e^{-kt}$ where

$$k = k_1 K_0 [\text{M}] / (1 + K_0 [\text{M}]) \quad (1)$$

In this equation, $[\text{M}]$ represents the free metal ion concentration (Mg^{2+} or Al^{3+}) and k_1 is the rate constant for addition of M-

containing protomer with a stability constant (K_0) to be designated below. In these experiments, the total tubulin concentration was held constant. A point-by-point analysis along the entire course of a turbidity-versus-time curve in the presence of M (Fig. 1) showed an excellent fit to the form of the equation for turbidity. Analysis also revealed that to obtain estimates of the initial elongation rates in the presence of an interfering initiation phase, it was necessary to analyze the steepest possible slope of the plot for turbidity versus time. The slope is proportional to k in Eq. 1, which represents a saturation binding curve. The apparent K_0 was evaluated by a nonlinear least-squares fit of the observed initial rate (k) versus added M concentration $[\text{M}]$.

The concentration of metal ion was set by

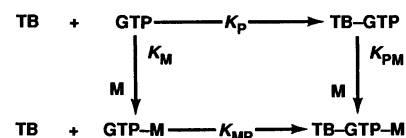
a metal ion-containing buffer with variable amounts of excess ligand. Free metal ion concentrations were evaluated by the use of Eq. 2

$$[\text{M}] = [1 + (\text{H}^+)/K_a]R / (1 - R)K_s [1 + K_b/(\text{H}^+)] \quad (2)$$

The free Al^{3+} concentration when nitrilotriacetate (NTA) was used as ligand was calculated as follows. The logarithm of the acidity constant ($\text{p}K_a$) for the protonated ligand is 9.58, the logarithm of the stability constant ($\log K_s$) for Al^{3+} and NTA is 11.37, the logarithm of the basicity constant ($\text{p}K_b$) for Al^{3+} hydrolysis in the complex is 5.22 (13), and R is the molar ratio of total $[\text{Al}^{3+}]$ to total $[\text{NTA}]$. (To complex any adventitious Ca^{2+} , 10 μM EGTA was present.) From this analysis, we found that the $\log K_0$ for Al^{3+} with the GTP-tubulin complex was 11.8. Since the GTP present could compete with NTA for chelation to Al^{3+} , we determined a stability constant ($\log K_s$ for the Al^{3+} -GTP complex). By allowance for Al^{3+} -hydroxo complex formation (14), we recalculated $\log K_s$ to be 10.9 from a reported conditional stability constant ($\log K_c = 6.2$) determined by a kinetic method at $\text{pH} = 6.95$ (15). Inclusion of GTP binding of Al^{3+} in the NTA analysis increases the $\log K_0$ value for Al^{3+} with the GTP-tubulin complex by only 0.2 log unit. The free Mg^{2+} concentrations were calculated from a stability constant with GTP of $\log K_s = 4.2$ and $\text{p}K_a = 6.5$ for the triphosphate group (16). No NTA was present in the Mg^{2+} experiments, and, under the experimental conditions, EGTA does not compete with GTP for Mg^{2+} .

The results are summarized in Table 1. The $\log K_0$ values derived from a fit to Eq. 1 over a range of calculated free metal ion concentrations gave a standard deviation of less than 0.1 unit in the nonlinear least-squares analysis. Examination of the data in Table 1 revealed that the $\log K_0$ value for Al^{3+} is 7.5 units stronger than that for Mg^{2+} . For both metal ions, the kinetically derived $\log K_0$ values exceed the $\log K_M$ values (see below) for association of the metal ion with GTP.

Two possible pathways for formation of the microtubule elongating species (TB-GTP-M) from tubulin (TB), GTP, and metal ion (M) are considered in the following scheme:



The four equilibrium constants (K_P , K_M , K_{PM} , and K_{MP}) are defined as association

constants for the pathways leading to ternary complex TB-GTP-M of Eq. 2 in the directions indicated by the arrowheads. For the cyclic system, $K_P K_{PM} = K_M K_{MP}$. The total molar concentration of tubulin, $[TB_{total}]$, is given by

$$[TB_{total}] = [TB_{free}] + [TB-GTP] + [TB-GTP-M] \quad (3)$$

from which the molar concentration of ternary complex is $[TB-GTP-M] = [TB_{total}] / D$, where $D = 1 + 1/K_{PM}[M] + 1/K_P K_{PM}[M][GTP]$. The last term in the denominator will be less than the penultimate term if $K_P[GTP] \gg 1$. Since $[GTP]$ is in the millimolar range, and we expect $K_P > 10^4$, the condition prevails. In addition, no $[GTP]$ dependence of the rate is observed experimentally. In terms of the cyclic scheme, the initial rate constant for appearance of microtubule polymer in the elongation phase is given by

$$k = k_2[TB-GTP-M] = k_2[TB_{total}]K_{PM}[M]/(1 + K_{PM}[M]) \quad (4)$$

This equation is identical in form to Eq. 1, with $k_1 = k_2 [TB_{total}]$ and K_0 , the apparent stability constant of Eq. 1, equal to K_{PM} . Thus, we identify the kinetically determined K_0 with the stability constant, K_{PM} , for association of free metal ion with the tubulin-GTP complex. This identification accounts for the greater values of K_0 over K_M in Table 1 for both Mg^{2+} and Al^{3+} .

Identification of the kinetically determined stability constant K_0 to metal ion association with the GTP-tubulin complex receives support from an entirely different approach. In an equilibrium study with the Mn^{2+} concentration determined by electron paramagnetic resonance, Mn^{2+} became associated with a single high-affinity site (identified as the exchangeable nucleotide-binding site) on GTP-tubulin with $\log K_{PM} = 5.9$ (17). Magnesium ion competes with Mn^{2+} binding at this site, and, from the conditions described, we calculate that for Mg^{2+} , $\log K_{PM} \sim 4.7$. This value agrees well with $\log K_0 = 4.5$ determined kinetically for tubulin polymerization.

Correlation of K_0 with K_{PM} in the cyclic system, with prior knowledge of K_M , establishes the ratio $K_{PM}/K_M = K_{MP}/K_P \approx 2$ for Mg^{2+} and ≈ 13 for Al^{3+} . The additional determination of $\log K_{MP} = 7.7$ with Mg^{2+} (18) allows estimation of all four equilibrium constants. Thus, we conclude that for GTP binding to tubulin in the absence of any metal ion, $\log K_P = 7.4$. In turn, this result combined with those in Table 1, leads to $\log K_{MP} = 8.5$ for Al^{3+} .

Accurate assessment of our findings in the etiology or pathophysiology of Al^{3+} -mediated disease states would require a thorough

knowledge of the mechanisms that regulate the functioning of microtubules in vivo (6). Nonetheless, elevated concentrations of Al^{3+} could interfere with microtubule function and regulation by several potential mechanisms.

Tubulin has been reported to bind two molecules of guanine nucleotide: one, exclusively a GTP, is bound at a nonexchangeable site, and another, either a GDP or a GTP, is bound at an exchangeable (E) site, which undergoes facile exchange with free nucleotide (12, 19). Occupancy of the E site with GTP in a process linked with the binding of Mg^{2+} is required for tubulin polymerization (6, 9, 17, 20). After the polymerization of M-GTP-bound tubulin monomers into microtubules, the bound GTP becomes hydrolyzed to GDP, which has been suggested to differentiate the assembly (M-GTP bound) and disassembly ends (M-GDP bound) of the microtubule (21). Upon dissociation of the microtubule into tubulin monomers, GDP undergoes exchange with GTP, enabling the next cycle of microtubule assembly. Thus, GTP hydrolysis and GDP-GTP exchange are essential processes in the normal regulation of microtubule assembly and disassembly.

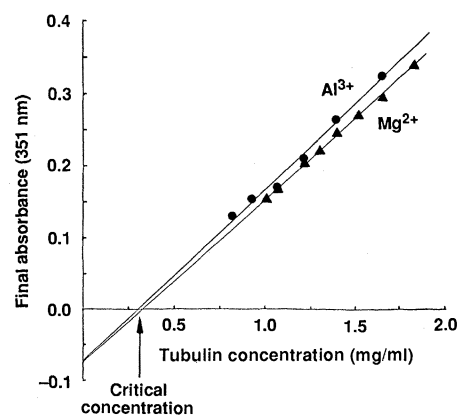


Fig. 3. An example of a determination of the critical concentrations for tubulin polymerization promoted by Al^{3+} and Mg^{2+} . The initial tubulin assembly conditions were as follows: MAP-free tubulin (20 μM), GTP (1.0 mM), Pipes (0.1M), DMSO (8% by volume), and either Mg^{2+} (\blacktriangle , 1.0 mM) or Al^{3+} (\bullet , $4.0 \times 10^{-11} M$). Serial dilutions of the polymerized samples with the metal ion-GTP-Pipes-DMSO buffer produced the designated protein concentrations with the corresponding absorbance values. The critical concentrations for these systems in vitro supported by Al^{3+} and Mg^{2+} were 0.28 ± 0.05 and 0.30 ± 0.05 mg/ml, which represent the averages of two duplicate experiments.

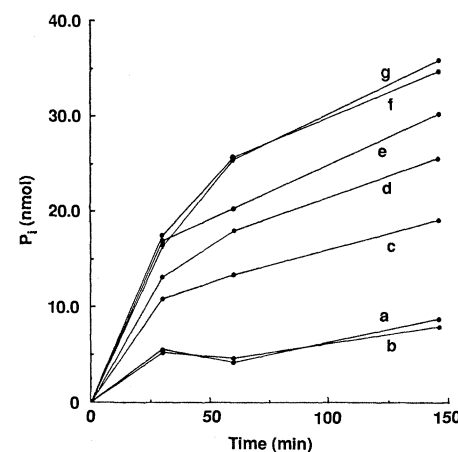


Fig. 4. A comparison of the rates of γ - $[^{32}P]$ GTP hydrolysis for Al^{3+} -promoted and Mg^{2+} -promoted microtubules. The polymerization conditions were as follows: MAP-free tubulin (30 μM), GTP (0.1 mM), Pipes (0.1M), DMSO (8% by volume), and the designated metal ion concentrations. A standardized free Al^{3+} concentration of $4.0 \times 10^{-10} M$ [produced by buffering a 50 μM $AlCl_3$ solution with NTA (55 μM)] was present in all incubations except those depicted by curves a and g. The plots represent the following metal ion concentrations: curve a, no metal ion present; curve b, Al^{3+} ; curve c, Al^{3+} and Mg^{2+} (50 μM); curve d, Al^{3+} and Mg^{2+} (100 μM); curve e, Al^{3+} and Mg^{2+} (200 μM); curve f, Al^{3+} and Mg^{2+} (1.00 mM); and curve g, Mg^{2+} (1.00 mM). Microtubule formation as monitored by absorption at 351 nm was complete within 10 to 15 minutes and remained within 10% of maximal absorption throughout the course of the experiments depicted in plots b through g; no initial microtubule formation and slow tubulin decomposition over the course of the experiment was observed in experiment a.

We have demonstrated that Al^{3+} -GTP microtubules undergo GTP hydrolysis significantly more slowly than their Mg^{2+} -GTP counterparts (less than 1/100 as fast) (22) (Fig. 4, curves b and g). Using GTP hydrolysis as a probe of microtubule metal ion content, we found that Al^{3+} at a concentration of $4.0 \times 10^{-10} M$ can supplant Mg^{2+} in the polymerization of MAP-free tubulin in vitro when Mg^{2+} concentrations fall below 1.0 mM (Fig. 4). Thus, aberrant homeostasis of Mg^{2+} concentrations (of less than about one-fifth those expected in vivo) might result in Al^{3+} -supported tubulin po-

Table 1. Stability constant logarithms for tubulin polymerization (K_0), GTP-binding (K_M), and the metal ion-GTP-tubulin ternary complex ($K_M K_{MP}$). The stability constants for K_0 were determined experimentally and have standard deviations of less than 0.1 unit; the stability constants for K_M and $K_P K_{PM}$ are derived by calculation from literature values and have undefined error terms (in the range $\pm <0.3$ unit).

Metal ion	$\log K_0$ (M^{-1})	$\log K_M$ (M^{-1})	$\log K_P K_{PM}$ (M^{-2})
Mg^{2+}	4.5 ± 0.1	4.2 (16)	11.9
Al^{3+}	12.0 ± 0.1	10.9 (14)	19.4

lymerization and the attenuation of the Mg^{2+} -dependent mechanisms regulating microtubule assembly, since Al^{3+} concentrations and total aluminum burdens in these ranges become relevant under pathological conditions (1). In addition, the exchange of guanine nucleotides (GTP for GDP) would also be expected to be slower when Al^{3+} is associated in the GTP-tubulin ternary complex, because of the extremely slow rate of ligand exchange of Al^{3+} (about 10^{-5} the rate of that of Mg^{2+}) (23).

Tubulin polymerization and microtubule stability are sensitive to Ca^{2+} in vitro and in vivo, with elevated concentrations inhibiting tubulin polymerization and promoting microtubule depolymerization (24). The Al^{3+} microtubules were less sensitive with regard to both rate and extent of Ca^{2+} -induced depolymerization than Mg^{2+} -microtubules, and Al^{3+} (at $4.0 \times 10^{-11}M$) polymerizes significantly more tubulin in the presence of elevated Ca^{2+} concentrations than the Mg^{2+} -supported system (at 1.0 mM) (25). This result is presumably a consequence of the enhanced association constant of the Al^{3+} -GTP-tubulin complex relative to its Mg^{2+} counterpart and the mechanism of Ca^{2+} -mediated depolymerization in vitro (24); it is also consistent with slower microtubule treadmilling for Al^{3+} -microtubules relative to Mg^{2+} -microtubules.

Thus, Al^{3+} might disrupt the sensitive dynamics and thermodynamics of microtubule formation and disassembly in vivo through the inhibition of GTP hydrolysis and nucleotide exchange, as well as through a depressed sensitivity to regulation of polymerization and depolymerization processes by Ca^{2+} . In addition, Al^{3+} incorporation could affect the tertiary structure of the microtubule polymer, as well as the tubulin monomer, through the maintenance of GTP-M-bound subunits. The physiological impact of such subtle changes in microtubule structure might be manifested in altered interactions with the multiplicity of microtubule-associated proteins known to associate with both the monomeric and the polymeric tubulin subunits.

These findings may have implications for other GTP-binding proteins, which include nucleotide-binding enzymes, signal-transducing G proteins, and the product of the *ras* oncogene (26). The three-dimensional structures of two of these proteins incorporate a Mg^{2+} at the nucleotide-binding site (27). In several of these proteins, GTP hydrolysis and GDP-GTP exchange serve as critical control mechanisms (26, 27). The competition between Mg^{2+} and Al^{3+} may affect the normal function of these proteins in vivo.

REFERENCES AND NOTES

- P. O. Ganrot, *Environ. Health Perspect.* **65**, 363 (1986); M. R. Wills and J. Savory, *Lancet* **1983-II**, 29 (1983); I. S. Parkinson, M. K. Ward, D. N. S. Kerr, *J. Clin. Pathol.* **34**, 1285 (1981).
- D. C. Gajdusek, *N. Engl. J. Med.* **312**, 714 (1985); D. P. Perl, D. C. Gajdusek, R. M. Garruto, R. T. Yanagihara, C. J. Gibbs, Jr., *Science* **217**, 1053 (1982).
- D. P. Perl and A. R. Brody, *Science* **208**, 297 (1980); D. R. Crapper, S. S. Krishnan, A. J. Dalton, *ibid.* **180**, 511 (1973); see also: R. J. Wurtman, *Sci. Am.* **252**, 62 (January 1985); J. T. Coyle, D. L. Price, M. R. DeLong, *Science* **219**, 1184 (1983).
- R. P. Hooper and C. A. Shoemaker, *Science* **229**, 463 (1985); C. T. Driscoll *et al.*, *Nature (London)* **284**, 161 (1980); C. S. Cronan and C. L. Schofield, *Science* **204**, 304 (1979).
- J. C. Troncoso *et al.*, *Brain Res.* **342**, 172 (1985); K. S. Kosik *et al.*, *Neurochem. Pathol.* **3**, 99 (1985); A. Bizzi *et al.*, *J. Neurosci.* **4**, 722 (1984); J. C. Troncoso *et al.*, *Ann. Neurol.* **12**, 278 (1982).
- P. Dustin, *Microtubules* (Springer-Verlag, New York, 1984), chap. 3, pp. 94-126; A. C. Rosenfeld, R. V. Zackroff, R. C. Weisenberg, *FEBS Lett.* **65**, 144 (1976).
- R. C. Williams, Jr., and E. Lee, *Methods Enzymol.* **85**, 376 (1982).
- H. W. Detrich III and R. C. Williams, Jr., *Biochemistry* **17**, 3900 (1978).
- R. H. Himes, P. R. Burton, J. M. Gaito, *J. Biol. Chem.* **252**, 6222 (1977).
- F. Gaskin, C. R. Cantor, M. L. Shelansky, *J. Mol. Biol.* **89**, 737 (1974).
- B. J. Berne, *ibid.*, p. 755.
- D. L. Purich and D. Kristofferson, *Adv. Protein Chem.* **36**, 133 (1984).
- T. R. Bhat, R. R. Das, J. Shankar, *Indian J. Chem.* **5**, 324 (1967).
- R. B. Martin, *Clin. Chem.* **32**, 1797 (1986).
- R. E. Viola, J. F. Morrison, W. W. Cleland, *Biochemistry* **19**, 3131 (1980).
- H. Sigel, *J. Inorg. Nucl. Chem.* **39**, 1903 (1977).
- D. K. Jemiole and C. M. Grisham, *J. Biol. Chem.* **257**, 8148 (1982).
- B. Zeeberg and M. Caplow, *Biochemistry* **18**, 3880 (1979); J. L. Fishback and L. R. Yarbrough, *J. Biol. Chem.* **259**, 1968 (1984).
- J. J. Correia and R. C. Williams, Jr., *Annu. Rev. Biophys. Bioeng.* **12**, 211 (1983).
- R. B. Maccioni and N. W. Seeds, *J. Biol. Chem.* **257**, 3334 (1982); J. C. Lee and S. N. Timasheff, *Biochemistry* **16**, 1754 (1975).
- M. Caplow and R. Reid, *Proc. Natl. Acad. Sci. U.S.A.* **82**, 3267 (1985); T. Mitchison and M. Kirschner, *Nature (London)* **312**, 237 (1984); M.-F. Carlier, T. L. Hill, Y.-C. Chen, *Proc. Natl. Acad. Sci. U.S.A.* **81**, 771 (1984).
- For examples of the inhibition of enzymatic adenosine triphosphate hydrolysis by Al^{3+} , see G. A. Trapp [*Kidney Int.* **29** (Suppl. 18), S-12 (1986)], E. Bellorin-Font *et al.* [*Endocrinology* **117**, 1456 (1985)], L. P. Solheim and J. J. Fromm [*Biochemistry* **19**, 6074 (1980)], and F. C. Womack and S. P. Colowick [*Proc. Natl. Acad. Sci. U.S.A.* **76**, 5080 (1979)].
- H. Diebler *et al.*, *Pure Appl. Chem.* **20**, 93 (1969).
- R. C. Weisenberg and W. J. Deery, *Biochem. Biophys. Res. Commun.* **102**, 924 (1981); M. Schliwa *et al.*, *Proc. Natl. Acad. Sci. U.S.A.* **78**, 1037 (1981); T. L. Karr *et al.*, *J. Biol. Chem.* **255**, 11,853 (1980).
- T. L. Macdonald and W. G. Humphreys, unpublished results.
- A. Gilman, *Cell* **36**, 577 (1984); J. B. Hurley, M. I. Simon, D. B. Teplow, J. D. Robishaw, A. G. Gilman, *Science* **226**, 860 (1984); P. C. Sternweis and A. G. Gilman, *Proc. Natl. Acad. Sci. U.S.A.* **79**, 4888 (1982).
- F. Jurnak, *Science* **230**, 32 (1985); F. McCormick *et al.*, *ibid.*, p. 78.
- We thank L. Rebhun for insightful comments and assistance. Supported through NIH grants AM 32453 and ES 03181.

22 September 1986; accepted 23 January 1987

First Record of Giant Anteater (*Xenarthra*, *Myrmecophagidae*) in North America

CHRISTOPHER A. SHAW AND H. GREGORY McDONALD

A right metacarpal III represents the first North American record of the giant anteater (*Myrmecophaga tridactyla*). Recovered in northwestern Sonora, Mexico, with a rich vertebrate fauna of early Pleistocene (Irvingtonian) age, it belongs to a cohort of large mammals that dispersed from South America to North America along a savanna corridor. Presumably habitat and climatic changes have subsequently driven this mammalian family more than 3000 kilometers back into Central America from its former expansion into temperate North America.

NEW WORLD ANTEATERS (VERMI-lingua) occur rarely in the fossil record, and knowledge of their evolution and fossil distribution have had to be pieced together (1). The three extant genera of the family Myrmecophagidae are presently restricted to tropical Central and South America, and the four valid fossil genera are also confined to South America. Therefore, discovery of the giant anteater (*Myrmecophaga tridactyla*) in the early Pleistocene of northernmost Mexico, more than 3000 km north of its present range, was unexpected (Fig. 1).

The fossil specimen, a complete right metacarpal III of an adult animal (Fig. 2),

was recovered from the surface of (unnamed) nonmarine sediments to the northeast of El Golfo de Santa Clara, Sonora, Mexico (31°40'N, 114°30'W). It is identical in morphology, size, and proportions to the metacarpal III of modern *Myrmecophaga tridactyla*. This distinctive skeletal element, with its deep distal keel, supports the largest and most powerful digging claw that is used to open termite mounds and is quite diagnostic for this species.

C. A. Shaw, George C. Page Museum, Los Angeles, CA 90036.

H. G. McDonald, Cincinnati Museum of Natural History, Cincinnati, OH 45202.